Multiple wavelength Fabry–Pérot lasers fabricated by vacancy-enhanced quantum well disordering

D. Hofstetter,[a)] H. P. Zappe, J. E. Epler, and P. Riel
Paul Scherrer Institut Zürich, Badenerstrasse 569, CH-8048 Zürich, Switzerland

Wavelength-shifted GaAs/AlGaAs Fabry–Pérot ridge waveguide lasers were fabricated by vacancy-enhanced quantum well disordering using dielectric cap annealing. 500 μm long and 4 μm wide Fabry–Pérot lasers with emission wavelengths selectively shifted by 20 nm were integrated with unshifted lasers on the same chip, characterized and further compared with lasers fabricated from as-grown material. These investigations showed that the absorption edge of a single-quantum well double heterostructure can be selectively blueshifted after epitaxial growth without compromising diode laser performance.

Postgrowth control of a quantum well (QW) profile has important applications for monolithic integration of active and passive optoelectronic components. A straightforward realization of many concepts in integrated optoelectronics requires a postgrowth conversion of a semiconductor heterostructure into a pattern of transparent and absorbing regions. The absorbing sections become light sources and detectors while the transparent regions could be low-loss waveguides, phase modulators, or distributed Bragg reflectors. The most promising processes are based upon a local partial intermixing of a quantum well to blueshift the energy band gap by several tenths of nm. Demonstrated techniques include impurity-induced disordering using various impurity species[1,2] and vacancy-enhanced disordering (VED).[1–7] VED by dielectric cap annealing has the advantage that only partial intermixing occurs, leaving waveguiding structures intact, and that the electrical properties of the material are not strongly affected. Recently, VED has been used to blueshift the absorption edge of the grating section of a DBR laser.[8] However, threshold currents were increased by either Zn diffusion into the active layer[9,10] or a mismatch between Bragg peak of the grating and gain peak of the material raising doubts about the applicability of the process. Our results indicate that VED can be employed in integrated optoelectronics without the drawbacks listed above. In this letter we describe the use of VED to locally shift the band gap of a single-QW separate-confinement double heterostructure. Ridge waveguide Fabry–Pérot lasers were fabricated from unshifted and shifted sections on the same laser bar. Both showed cw output powers up to 12 mW per facet, threshold currents less than 14 mA and a slope efficiency of 0.42 W/A. These values are comparable with those of unannealed devices fabricated from the same material.

The layer structure for these experiments was a MOVPE-grown separate-confinement double heterostructure grown on an *n*-type, Si-doped (10^{18} cm^{-3} Si) GaAs substrate and consisted of the following layers: a 1.1 μm thick $Al_{0.8}Ga_{0.2}As$ lower cladding layer (*n*-doped 1.5×10^{18} cm^{-3} Si), an undoped 165 nm thick $Al_{0.3}Ga_{0.7}As$ core containing a single GaAs QW (7 nm) and an 0.8 μm thick $Al_{0.8}Ga_{0.2}As$ upper cladding layer (*p*-doped 10^{18} cm^{-3} Mg) covered with a 100 nm thick highly *p*-doped 10^{18} cm^{-3} (8×10^{18} cm^{-3} Zn) GaAs cap layer.

Dielectric cap annealing, which is used for the VED, has been described extensively in Refs. 5 and 9; therefore, we will give only a brief introduction. Using standard processing techniques, the sample was completely covered with a single layer of either e-beam evaporated SiO_2 or thermally evaporated SrF_2. During rapid thermal annealing (RTA) at 960 °C for 30 s, group-III vacancies are generated under the SiO_2 cap, but not under the SrF_2 cap. Under the SiO_2, the vacancies promote intermixing of the Ga in the GaAs quantum well with column-III atoms [Al,Ga] of the adjacent $Al_{0.3}Ga_{0.7}As$ core, thereby increasing the effective Al content and the energy band gap of the QW. Transmission electron microscope pictures of such intermixed quantum wells fabricated in this material system are shown in Ref. 11. Figure 1 shows the achievable blueshifts of the photoluminescence spectrum excited with an argon-ion laser ($\lambda=488$ nm, $P=10$ mW) and measured at room temperature. After RTA of 30, 60, and 90 duration, at temperatures between 910 and

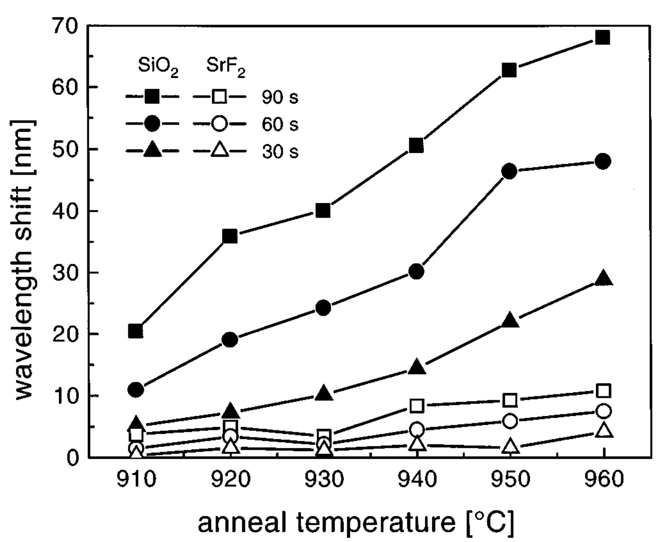

FIG. 1. Photoluminescence wavelength shift of SiO_2-capped and SrF_2-capped material after vacancy-enhanced disordering at different anneal temperatures and anneal times.

a)Electronic mail: hofstetter@psi.ch

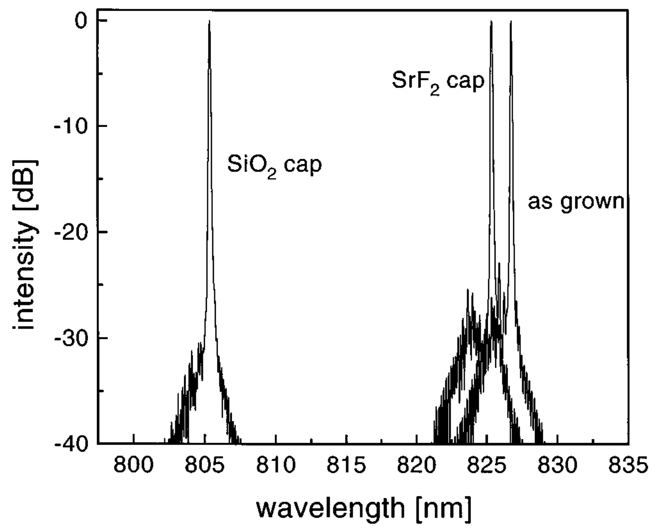

FIG. 2. Optical spectra of SiO_2-capped, SrF_2-capped, and as-grown material Fabry–Pérot lasers.

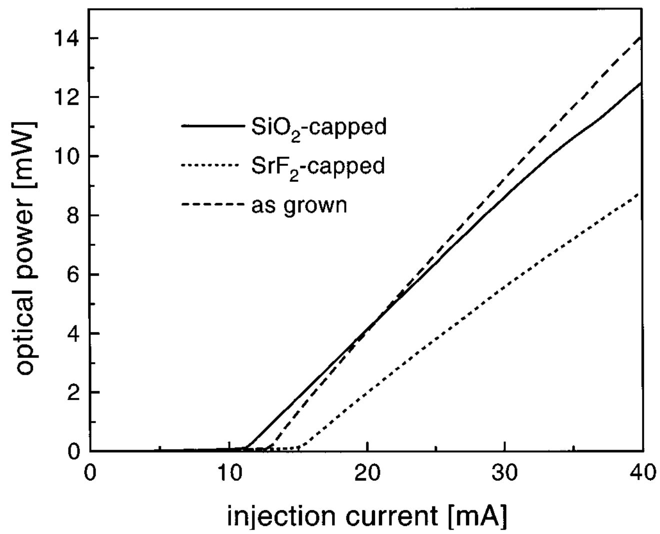

FIG. 3. L–I curves of SiO_2-capped, SrF_2-capped, and as-grown material Fabry–Pérot lasers.

960 °C, we measured blueshifts of the photoluminescence spectrum of 25 to 70 nm under the SiO_2 cap and less than 10 nm under the SrF_2 cap.

Lasers were then fabricated in both the shifted and the unshifted regions and in as-grown material. The process has been described previously[12] and is based upon dry etching of 4 μm wide ridges to within 100 nm of the waveguide core. 250 nm of Si_3N_4 was used as a passivating and electrically isolating layer on the shoulders and the sidewalls of the ridges. The material was cleaved into 500 μm long bars containing shifted and unshifted areas. The different types of lasers were separated by 250 μm and were tested unbonded in bar form, under cw conditions and at room temperature.

Figure 2 shows the emission spectra of three representative lasers driven cw above threshold, all at approximately the same current density. The as-grown, SrF_2-, and SiO_2-capped devices exhibit a peak spontaneous emission of 826, 823, and 805 nm, respectively; i.e., wavelength shifts of 3 and 21 nm. The corresponding photoluminescence wavelength shifts measured in this material are 2 and 19 nm ($\lambda_{\text{initial}}=812$ nm). These values are slightly smaller than those of the corresponding photoluminescence spectra (triangles at 960 °C in Fig. 1) because of the shorter anneal time (24 s instead of 30 s). The lasing wavelengths are located at or 1 nm to the long wavelength side of the spontaneous emission peak, typical for our Fabry–Pérot lasers. All devices are single mode with a side mode suppression ratio of 20 dB when driven at $I=3\times I_{\text{th}}$.

In Fig. 3 are shown the cw light versus current (L–I) data for the three devices of Fig. 2. The as-grown laser had a threshold current of 12 mA ($J_{\text{th}}=600$ A/cm^2) and a slope efficiency of 0.52 W/A. A maximum output power of 14 mW at $I=4\times I_{\text{th}}$ was achieved. In comparison, the L–I curve of the SiO_2-capped laser had a lower threshold current of 10 mA ($J_{\text{th}}=500$ A/cm^2), while the SrF_2-capped device had a somewhat higher threshold current of 14 mA ($J_{\text{th}}=700$ A/cm^2). The slope efficiencies of the SiO_2-capped laser (0.42 W/A) and the SrF_2-capped laser (0.36 W/A) are lower then that of the as-grown laser. Measurements of several lasers of each type gave nearly identical results.

I–V curves of the three lasers are shown in Fig. 4. The characteristics of the as-grown and the SiO_2-capped lasers are comparable with threshold voltages, $V(I_{\text{th}})$, of 2.1 and 2.15 V and series resistances of 30 and 24 Ω, respectively. The higher threshold voltage of 3.3 V and series resistance of 37 Ω of the SrF_2-capped laser may be a result of a displaced p-n junction caused by dopant diffusion during the RTA. However, no evidence of Zn diffusion into the n side was observed in stain-etched cross sections of the material. Another possible cause is the exposure of the contact region of the SrF_2-capped devices during three plasma processes (SiO_2 patterning, SiO_2 strip and Si_3N_4 contact hole etch). The SiO_2-capped lasers experienced only one plasma exposure (Si_3N_4 contact hole etch). The higher threshold voltage

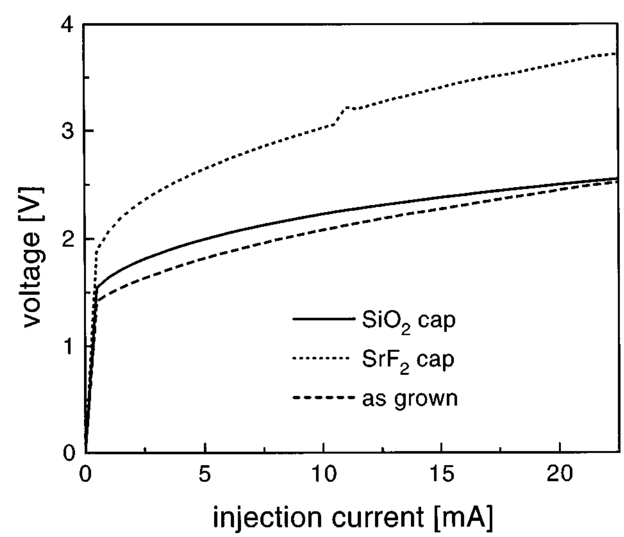

FIG. 4. I–V curves of SiO_2-capped, SrF_2-capped, and as-grown material Fabry–Pérot lasers.

and series resistance of the SrF_2-capped laser may explain the higher threshold current and reduced slope efficiency. Although no systematic lifetime measurements were done, we could not see any degradation of the laser performance during these measurements.

In conclusion, Fabry–Pérot lasers with two different emission wavelengths have been fabricated on the same bar. The wavelength shift of 20 nm was achieved through a post-growth process, vacancy-enhanced disordering. As opposed to earlier experiments,[9] the performance of these devices is comparable with that of as-grown material lasers. We could not see any Zn diffusion into the active region and furthermore, we were able to achieve cw operation of all our devices.

We are grateful to M. Moser and H. P. Schweizer for crystal growth, D. Jeggle and A. Vonlanthen for processing assistance, J. Söchtig for helpful discussions and H. W. Lehmann, M. T. Gale and R. Dändliker (IMT, University of Neuchâtel) for their generous support.

[1] G. F. Redinbo, H. G. Craighead, and J. M. Hong, J. Appl. Phys. **74**, 3099 (1993).

[2] R. L. Thornton, W. J. Mosby, and T. L. Paoli, J. Lightwave Technol. **6**, 786 (1988).

[3] D. G. Deppe, L. J. Guido, N. Holonyak, Jr., K. C. Hsieh, R. D. Burnham, R. L. Thornton, and T. L. Paoli, Appl. Phys. Lett. **49**, 510 (1986).

[4] J. H. Marsh, S. J. Hansen, A. C. Bryce, and R. M. De La Rue, Opt. Quantum Electron. **23**, 941 (1991).

[5] I. Gontijo, T. Krauss, J. H. Marsh, and R. M. De La Rue, IEEE J. Quantum Electron. **QE-30**, 1189 (1994).

[6] H. P. Zappe, D. Hofstetter, and H. E. G. Arnot, Proc. SPIE **2213**, 205 (1994).

[7] I. Gontijo, Y. S. Tang, R. M. De La Rue, C. M. Sotomayor Torres, J. S. Roberts, and J. H. Marsh, J. Appl. Phys. **76**, 5434 (1994).

[8] S. G. Ayling, J. Beauvais, and J. H. Marsh, *Proceedings of the 6th European Conference on Integrated Optics and Technical Exhibit* (ECIO, 1993), pp. 7–10.

[9] S. G. Ayling, A. C. Bryce, I. Gontijo, J. H. Marsh and J. S. Roberts, Semicond. Sci. Technol. **9**, 2149 (1994).

[10] S. O'Brien, J. R. Shealy, F. A. Chambers, and G. Devane, J. Appl. Phys. **71**, 1067 (1992).

[11] L. J. Guido, N. Holonyak, Jr., K. C. Hsieh, R. W. Kaliski, W. E. Plano, R. D. Burnham, R. L. Thornton, J. E. Epler, and T. L. Paoli, J. Appl. Phys. **61**, 1372 (1987).

[12] D. Hofstetter, H. P. Zappe, J. E. Epler, and J. Söchtig, Electron. Lett. **30**, 1858 (1994).